

Supporting Information

Fluorescence probes exhibit photoinduced structural planarization: sensing *in vitro* and *in vivo* microscopic dynamics of viscosity free from polarity interference

Cheng-Ham Wu^{1,‡}, Yi Chen^{1,‡}, Kyrylo A. Pyrshev^{3,5}, Yi-Ting Chen¹, Zhiyun Zhang^{1,2,*}, Kai-Hsin Chang¹, Semen O. Yesylevskyy^{4,5}, Alexander P. Demchenko^{3,6*} and Pi-Tai Chou^{1,*}

¹Department of Chemistry, National Taiwan University, Taipei 10607, Taiwan

²Key Laboratory for Advanced Materials and Institute of Fine Chemicals, East China University of Science & Technology, Shanghai 200237, P. R. China

³Palladin Institute of Biochemistry, National Academy of Sciences of Ukraine, Kyiv 01030, Ukraine

⁴Laboratoire Chrono Environnement UMR CNRS 6249, Université de Bourgogne Franche-Comté, 16 route de Gray, 25030 Besançon Cedex, France

⁵Institute of Physics, National Academy of Sciences of Ukraine, Kyiv 03028, Ukraine

⁶Yuriy Fedkovych National University, 58012 Chernivtsi, Ukraine

‡ C-H. Wu and Y. Chen are equally contributed to this work

Probe Design and Synthesis

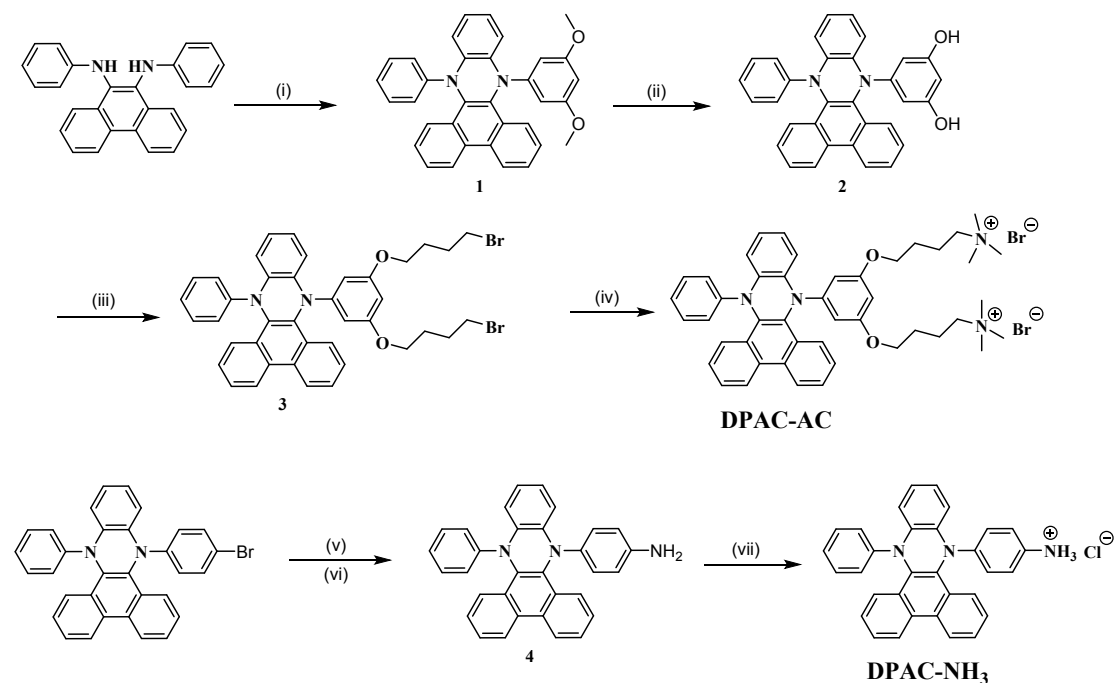


Figure S1. Synthesis procedure of molecules DPAC-AC and DPAC-NH₃.

(i) 1-iodo-3,5-dimethoxybenzene, K₂CO₃, Cu(CF₃SO₃)₂, 1,3,5-trichlorobenzene; (ii) BBr₃, DCM; (iii) 1,4-dibromobutane, K₂CO₃, acetonitrile; (iv) trimethylamine, THF; (v)

CuI, DMF, reflux; (vi) NaOH, EtOH, reflux; (vii) THF, HCl

9-(3,5-dimethoxyphenyl)-14-phenyl-9,14-dihydrodibenzo[*a,c*]phenazine (1)

Diphenylphenanthrene -9,10 -diamine (3.6 g, 10 mmol), 1-iodo-3,5-dimethoxybenzene (2.7 g, 10 mmol), K₂CO₃ (2.1 g, 15 mmol), Cu(CF₃SO₃)₂ (0.9 g, 2.5 mmol) and 1,3,5-trichlorobenzene (10 g) were added in a 100 mL flask. The mixture was heated to reflux and stirred under aerobic condition for 8 h. After cooling to room temperature, the solvent was removed by evaporation under reduced pressure to give residua. The solid was dissolved in dichloromethane and washed with saturate brine solution for three times. The organic solvent was evaporated and the obtained crude product was further purified by column chromatography on silica (petroleum ether: ethyl acetate = 30:1) to afford light yellow solid (2.5 g, 50%). ¹H NMR (400 MHz, DMSO-*d*₆, δ): 8.90 (d, J = 8.0 Hz, 2H), 7.97 (m, 2H), 7.86 (m, 2H), 7.69 (m, 2H), 7.62 (m, 2H), 7.38 (m, 2H), 7.09 (m, 2H), 6.95 (m, 2H), 6.82 (m, 1H), 6.14 (s, 2H), 6.04 (s, 1H), 3.45 (s, 6H).

5-(14-phenyldibenzo[*a,c*]phenazin-9(14*H*)-yl)benzene-1,3-diol (2)

To a dried flask was placed compound **1** (1.23 g, 2.5 mmol). The dried dichloromethane (20 mL) was added under N₂ atmosphere and the solution was cooled to 0 °C. BBr₃ (0.7 mL, 7.5 mmol) diluted in 10 mL dichloromethane was dropwise added into the mixture for 10 min, and then the mixture was warmed to room temperature overnight. Then the reaction was quenched by 100 mL water and extracted with dichloromethane, dried over MgSO₄. The combined organic layer was removed to give residua, which was further purified by column chromatography on silica (petroleum ether: ethyl acetate = 2:1) to afford solid (0.8 g, 69%). ¹H NMR (400 MHz, DMSO-*d*₆, δ): 8.94 (s, 2H), 8.90 (m, 2H), 8.01 (m, 1H), 7.88 (m, 2H), 7.73-7.54 (m, 5H), 7.37 (m, 2H), 7.07-7.02 (m, 4H), 6.85 (m, 1H), 5.86 (s, 2H), 5.66 (s, 1H).

9-(3,5-bis(4-bromobutoxy)phenyl)-14-phenyl-9,14-dihydrodibenzo[*a,c*]phenazine (3)

To a solution of compound **2** (0.47 g, 1 mmol) and 1,4-dibromobutane (0.32 g, 1.5 mmol) in acetonitrile (30 mL), K₂CO₃ (0.4 g, 3 mmol) was added. The mixture was heated to refluxed under N₂ atmosphere for 6 h. After cooling, the solvent was distilled under reduced pressure and the crude product was further purified by column chromatography on silica (petroleum ether: dichloromethane = 20:1) to afford light yellow solid (0.7 g, 95%). ¹H NMR (400 MHz, DMSO-*d*₆, δ): 8.90 (d, J = 8.0 Hz, 2H), 7.97 (m, 2H), 7.87 (m, 2H), 7.69 (m, 2H), 7.62 (m, 2H), 7.30 (m, 2H), 7.10 (m, 2H), 6.95 (m, 2H), 6.84 (m, 1H), 6.14 (s, 2H), 6.04 (s, 1H), 3.66(m, 4H), 3.46(m,4H), 1.77(m, 4H), 1.60 (m,4H). ¹³C NMR (100 MHz, DMSO-*d*₆, δ): 159.8,149.1,147.4,144.1,143.5,

137.1, 136.7, 129.4, 128.9, 128.3, 127.3, 126.9, 126.6, 125.8, 123.7, 123.6, 121.1, 116.4, 98.0, 94.9, 66.4, 34.7, 28.9, 27.1. HRMS(ESI) calcd. for $C_{40}H_{37}Br_2N_2O_2$: 737.1201 ($[M+H]^+$); found: 737.1204.

4,4'-((5-(14-phenyldibenzo[*a,c*]phenazin-9(14*H*)-yl)-1,3-phenylene)bis(oxy))bis(*N,N,N*-trimethylbutan-1-aminium) bromide (DPAC-AC)

To a solution of compound **3** (0.35 g, 0.8 mmol) in 30 mL tetrahydrofuran, trimethylamine (excess) was added. The mixture was stirred at 35 °C under N_2 atmosphere for 3 d. After cooling, the product was filtered and washed with tetrahydrofuran for several times to afford yellow solid (0.3 g, 75%). 1H NMR (400 MHz, $DMSO-d_6$) δ : 8.92 (d, $J = 8.0$ Hz, 2H), 7.97 (m, 2H), 7.87 (m, 2H), 7.69 (m, 2H), 7.63 (m, 2H), 7.41 (m, 2H), 7.10 (m, 2H), 6.95 (m, 2H), 6.84 (m, 1H), 6.16 (s, 2H), 6.07 (s, 1H), 3.68 (m, 4H), 3.24 (m, 4H), 3.15 (s, 18H), 1.67 (m, 4H), 1.53 (m, 4H). ^{13}C NMR (100 MHz, $DMSO-d_6$) δ : 159.8, 149.1, 147.3, 144.0, 143.6, 137.0, 136.8, 129.3, 129.1, 128.3, 127.4, 127.3, 127.2, 126.6, 125.8, 125.7, 123.7, 121.3, 116.6, 97.8, 94.9, 66.6, 64.8, 52.1, 25.4, 19.1. HRMS(ESI) calcd. for $C_{46}H_{54}Br_2N_4O_2$: 773.3430 ($[M-Br]^+$); found: 773.3433.

2-(4-(14-phenyldibenzo[*a,c*]phenazin-9(14*H*)-yl)phenyl)isoindoline-1,3-dione and 4-(14-phenyl adibenzo[*a,c*]phenazin-9(14*H*)-yl)aniline (4**)**

A mixture of 9-(4-bromophenyl)-14-phenyl-9,14-dihydrodibenzo[*a,c*]phenazine (0.26 g, 0.5 mmol), potassium phthalimide (0.11 g, 0.6 mmol) and CuI (0.057 g, 0.3 mmol) in DMF (20 mL) was heated to 80 °C and stirred under N_2 atmosphere for 8 h. After cooling to room temperature, the mixture was poured into water and filtered. The precipitate was washed with water and dichloromethane for several times to give crude product, which was used in the next reaction without further purification. To flask of obtained mixture, sodium hydroxide (0.04 g, 1 mmol) in ethyl alcohol (20 mL) was added. The reaction was refluxed for 5 h under N_2 atmosphere. After cooling to room temperature, the solvent was removed by evaporation and crude product was diluted in dichloromethane, washed with water and dried over $MgSO_4$. The combined organic layer was distilled to give residua, which was further purified by column chromatography on silica (hexane: EA = 1:3) to afford green solid (0.17 g, 77%). 1H NMR (400 MHz, $DMSO-d_6$) δ : 8.87 (d, $J = 8.0$ Hz, 2H), 8.03 (dd, $J = 12$ Hz, 8 Hz, 2H), 7.73 (m, 2H), 7.63 (m, 3H), 7.50 (m, 1H), 7.30 (m, 2H), 7.11 (m, 2H), 7.00 (d, $J = 12$ Hz, 2H), 6.87 (m, 3H), 6.34 (d, $J = 8$ Hz, 2H), 4.91 (s, 2H). ^{13}C NMR (100 MHz, $DMSO-d_6$) δ : 148.8, 146.0, 145.8, 141.3, 138.0, 136.8, 133.8, 129.8, 128.7, 128.3, 127.3, 126.7, 126.5, 126.1, 124.8, 124.1, 123.9, 123.5, 120.7, 115.9, 114.2. HRMS(ESI) calcd. for $C_{32}H_{24}N_3$: 450.1970 ($[M+H]^+$); found: 450.1967.

4-(14-phenyldibenzo[*a,c*]phenazin-9(14*H*)-yl)benzenaminium chloride (DPAC-NH₃)

To a solution of compound **4** (0.13 g, 0.3 mmol) in 15 mL tetrahydrofuran, hydrochloric acid (excess) was added. The mixture was stirred at room temperature under N₂ atmosphere overnight. The product was filtered and washed with tetrahydrofuran for several times to afford white solid (0.12 g, 86%).

¹H NMR (400 MHz, DMSO-*d*₆) δ: 9.47 (s, 3H), 8.94 (d, *J* = 8.0 Hz, 2H), 7.92 (m, 4H), 7.70 (m, 2H), 7.61 (m, 2H), 7.42 (m, 2H), 7.02 (m, 8H), 6.82 (m, 1H). ¹³C NMR (100 MHz, DMSO-*d*₆) δ: 147.3, 143.9, 143.7, 136.8, 128.5, 128.9, 128.3, 128.1, 127.3, 127.1, 126.7, 125.8, 125.7, 123.8, 123.7, 123.6, 121.4, 118.3, 116.9. HRMS(ESI) calcd. for C₃₂H₂₄N₃Cl: 450.1970 ([M-Cl]⁺); found: 450.1971.

Details of MD simulations of DPAC-OH in model DPPC membrane

The structures of the **DPAC-OH** molecule in the ground state were optimized in Gaussian09 (Frisch et al., 2009) at the B3LYP/6-31G level of theory. The topology was generated by Acypype topology generator (Sousa da Silva and Vranken, 2012). The ESP partial charges were computed and added to initial topology. The charges of topologically equivalent atoms were averaged.

The pre-equilibrated model DPPC lipid bilayer containing 128 lipid molecules was downloaded from the Slipids web site (<http://www.fos.su.se/~sasha/SLipids/Downloads.html>). The Slipids force field (Jämbeck and Lyubartsev, 2012) was used for lipids, which is one of the best force fields for the membrane systems available today (Palonciová et al., 2014). The AMBER99sb force field was used for the rest of the system. The dye was manually inserted into the bilayer and the system was equilibrated for 150 ns. Last 50 ns of the trajectories was used for analysis. The analysis was performed with Pteros molecular modeling library (Yesylevskyy, 2012; Yesylevskyy, 2015). VMD 1.9.3 (Humphrey et al., 1996) was used for visualization.

MD simulations were performed in Gromacs (Hess et al., 2008) versions 2016.1 and 2018.2 in the NPT ensemble at the pressure of 1 atm maintained by Berendsen barostat (Berendsen et al., 1984) with semi-isotropic pressure coupling. The Verlet cutoff scheme is used (Páll and Hess, 2013). Long range electrostatics was computed with the PME method (Van der Spoel et al., 2005). Velocity rescale thermostat (Bussi

et al., 2007) was used. The temperature of 320 K was used. An integration step of 2 fs was used in all simulations and all bonds were converted to rigid constraints.

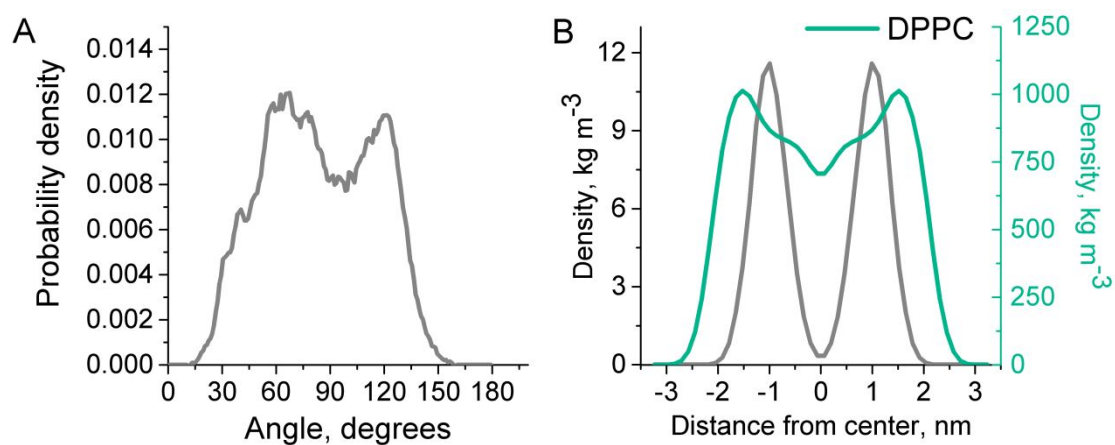


Figure S2. The data of MD simulations for DPAC-OH in model DPPC membrane.

(a) The distribution of the angles between the chromophore axis and the membrane normal. The chromophore axis is defined as the axis between its N atoms. (b) Density distribution of the lipids and the probe in the model membrane. The peaks show the most probable location of the probe in the membrane.

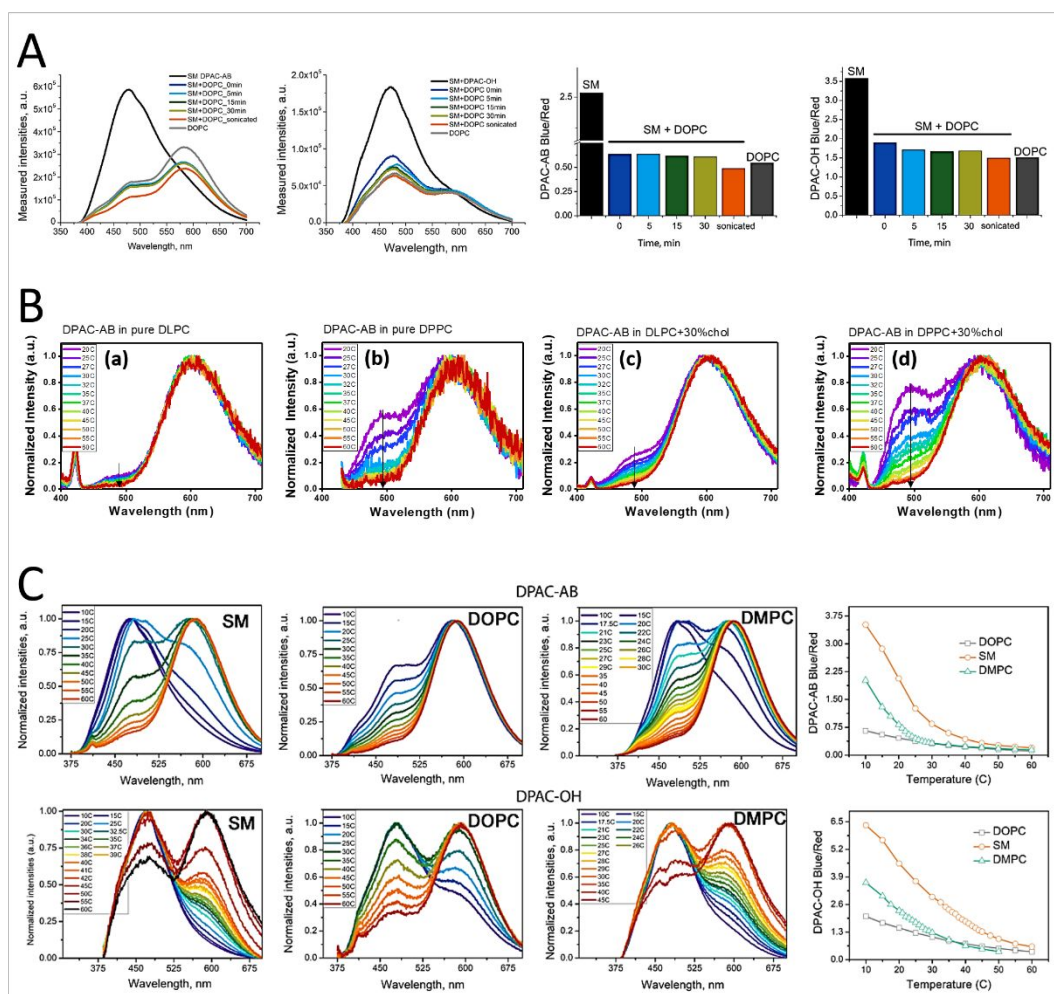


Figure S3. The spectral results of model membrane

A. Phase partitioning of DPAC dyes in membranes made of heterogeneous lipid mixtures. The fluorescent spectra of DPAC-AB and -OH and calculated blue/red ratio showing the probe redistribution toward the liquid-disordered phase in SUV. The probe was incorporated into the mixture of SM/DOPC, the spectra were measured during fixed periods of time and compared with pure SM and DOPC.

B. Spectral changes in membranes made of lipid mixtures on variation of temperature. Normalized emission spectra of DPAC-AB membrane probe in various lipid composition as a function of temperature. The probes were embedded into micelles (a,c) and vesicles (b,d) composed of phospholipids with different acyl chain lengths with or without cholesterol.

C. Normalized emission spectra of DPAC-AB and -OH membrane probes in various lipid composition and temperature, respectively. The probes were embedded into vesicles (SM, DOPC, DMPC) composed of phospholipids with different acyl chain lengths and their saturation. The λ -ratiometric analysis was applied to quantify the data and to compare the viscosity changes in different lipid systems.

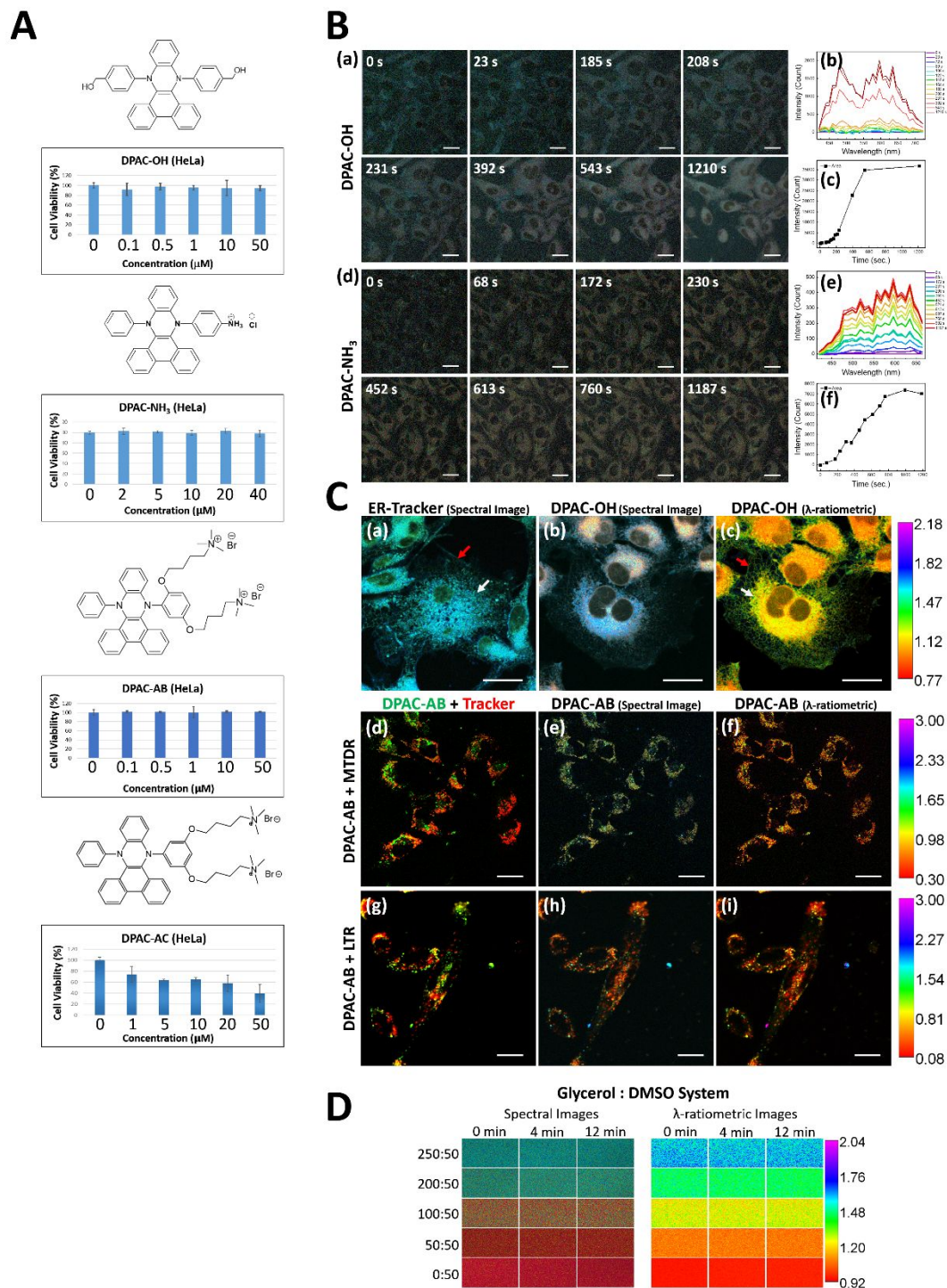


Figure S4. The results of *in vitro* cell studies:

A. Results of cell viability tests. Viability tests of HeLa cell treated with DPAC series. Cell viability tests were performed 5 times for each compound. A relatively low toxic concentration (1 μM) of the dye was used for *in vitro* and *in vivo* studies.

B. Internalization time of hydrophilic DPAC dyes. Time-lapse images of DPAC-OH and DPAC-NH₃ incorporated into HeLa cell. (a, d) Spectral time-lapse images, (b,

e) emission spectra of cells, and (c, f) the corresponding intensity at each time point. Excitation: 800 nm. Scale bar: 20 μm .

C. Results of co-localization studies. ER-Tracker Blue-white DPX (a) and **DPAC-OH** (b, c) labeled HeLa cells, respectively. ER-tracker and **DPAC-OH** were stained independently due to the overlapping emission. (Smooth ER: red arrow; rough ER: white arrow) Colocalization of **DPAC-AB** and mitoTracker Deep Red FM (MTDR, d, e, and f) and LysoTracker Red (LTR, g, h, and i). Emission of **DPAC-AB** is shown in false-color green, and mito- and LysoTracker is shown in red (d, g), respectively. The colocalized area (d, g) is shown in yellow or orange. Spectral images (e, h) and corresponding λ -ratiometric images of **DPAC-AB** were also presented in (f, i). Excitation: 800 nm (**-OH**, **-AB**, and ER-tracker), and 633 nm (MitoTracker Deep Red FM and LysoTracker Deep Red). Scale bar: 20 μm .

D. The spectral images and converted ratiometric images of DPAC dyes at various viscosities and laser exposure times. The spectral and ratiometric colors vary with viscosity changes; no changes are observed with increase of laser exposure time.

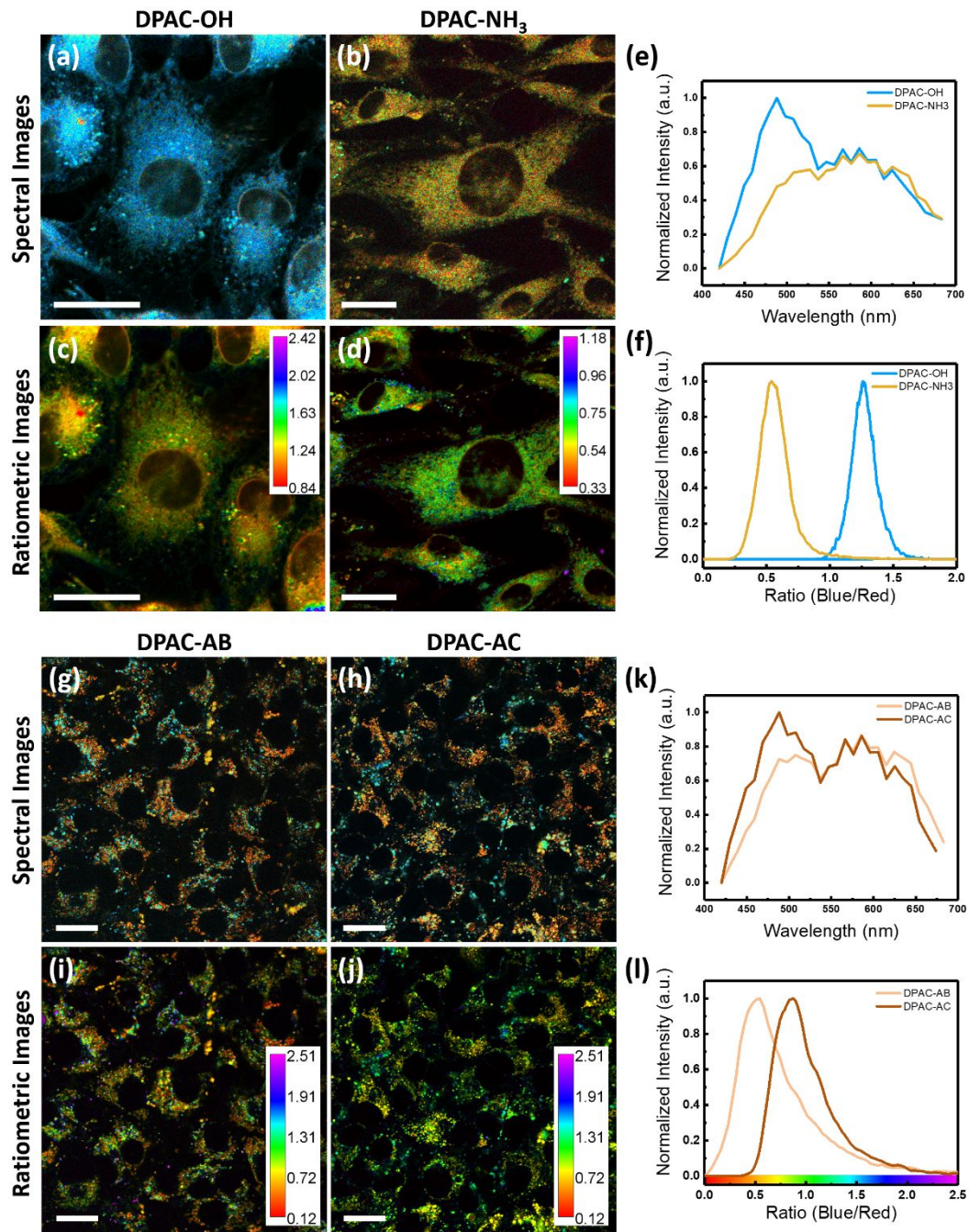


Figure S5. Microscopic Comparison of DPAC derivatives in Living Cells.

Spectral (a, b) and ratiometric (c, d) images of hydrophilic **DPAC-OH** and **DPAC-NH₃** labeled HeLa cells. The corresponding emission spectra of cell are shown in (e), and λ -ratiometric ($I_{480\text{nm}}/I_{600\text{nm}}$) histograms are shown in (f). Spectral (g, h) and λ -ratiometric (i, j) images of **DPAC-AB** and **DPAC-AC** labeled HeLa cells. The corresponding emission spectra of cell are shown in (k), and λ -ratiometric ($I_{480\text{nm}}/I_{600\text{nm}}$) histograms are shown in (l) as well. Excitation: 800 nm. Scale bar: 20 μm .

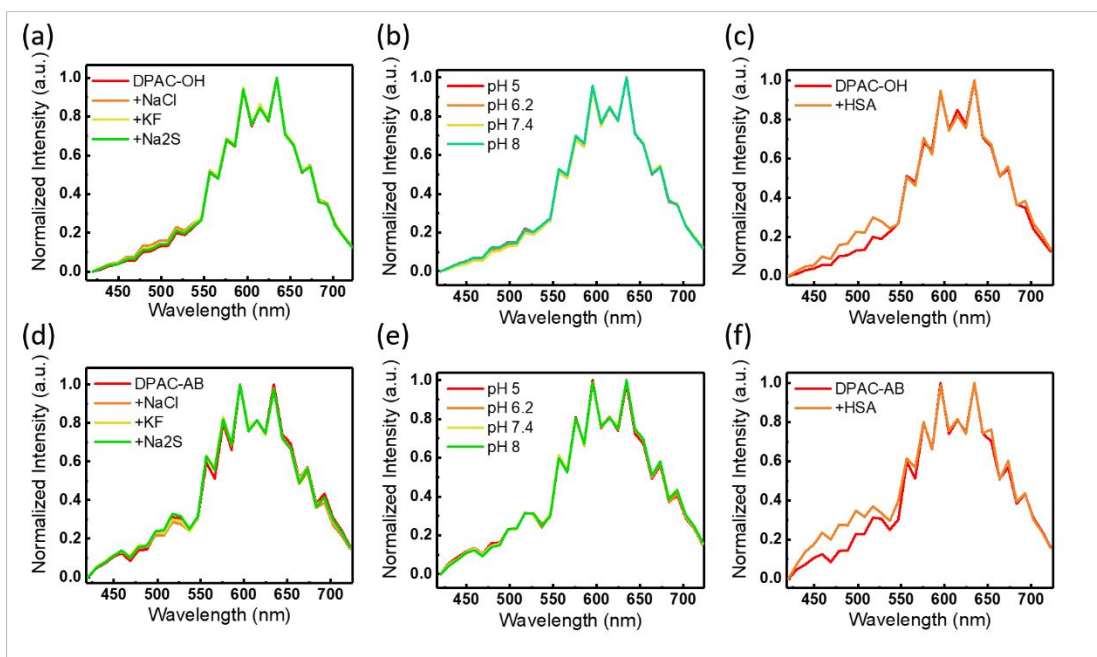


Figure S6. The spectral results of DPAC-OH and DPAC-AB in the (a, d) ion solutions, (b, e) the acid-based solution, and (c, f) the human serum albumin (HSA). (a, d) The concentration of ions (Na^+ , K^+ , and Cl^-) was prepared higher (500 mM) than the normal physiological condition of intra- and extracellular fluid. (b, e) The pH was adjusted to mimic biological conditions. (i.e. pH 5 for lysosome, pH 8 for mitochondria, and pH 6-7.4 for organelles and cytosol) (c, f) In the protein environment, no dramatically blueshift in emission spectra were observed. Slightly increasing in blue emission might be due to the slightly raise of viscosity by the HSA.

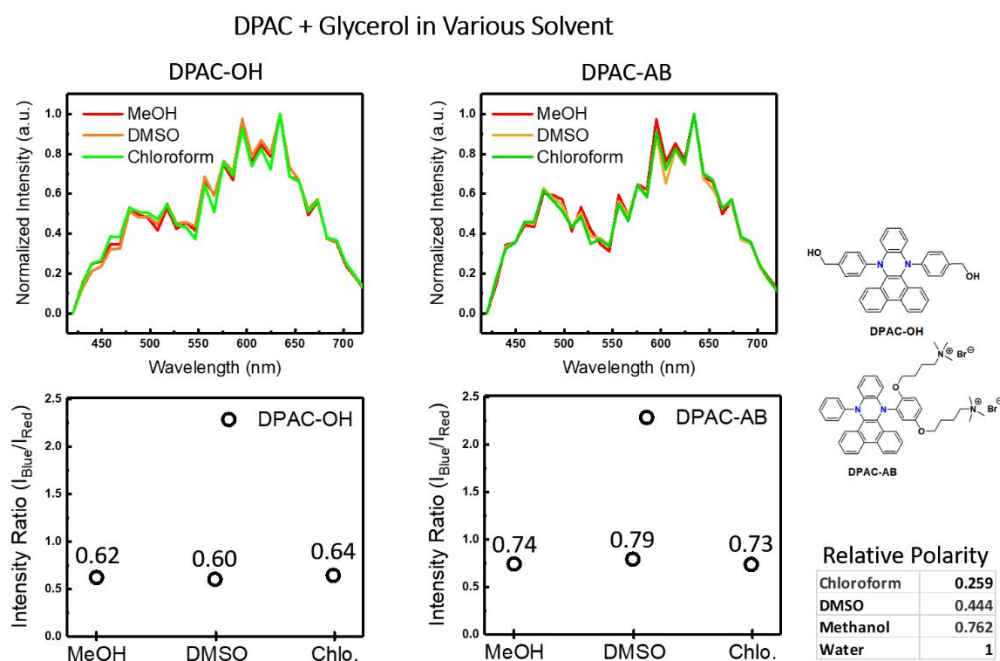


Figure S7. The test for solvent polarity effects on DPAC-OH and DPAC-AB. The solvent viscosity is prepared (v/v = 1:1) for the investigation of two emission bands. Results show the polarity-free behavior in both blue and red emissions for the DPAC-OH and DPAC-AB, respectively. No drastic alternation on the intensity ratio ($I_{480\text{nm}}/I_{600\text{nm}}$) is observed.

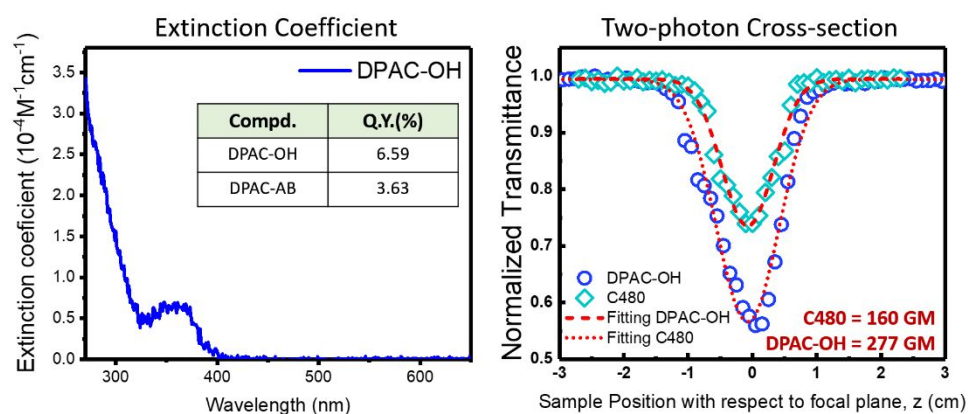


Figure S8. The photophysical properties of the DPAC-OH. DPAC-OH is dissolved in DMSO at the final concentration of 1 mM. The two-photon cross-section coefficient of DPAC-OH is measured to be 277 GM under the excitation of 800 nm laser.

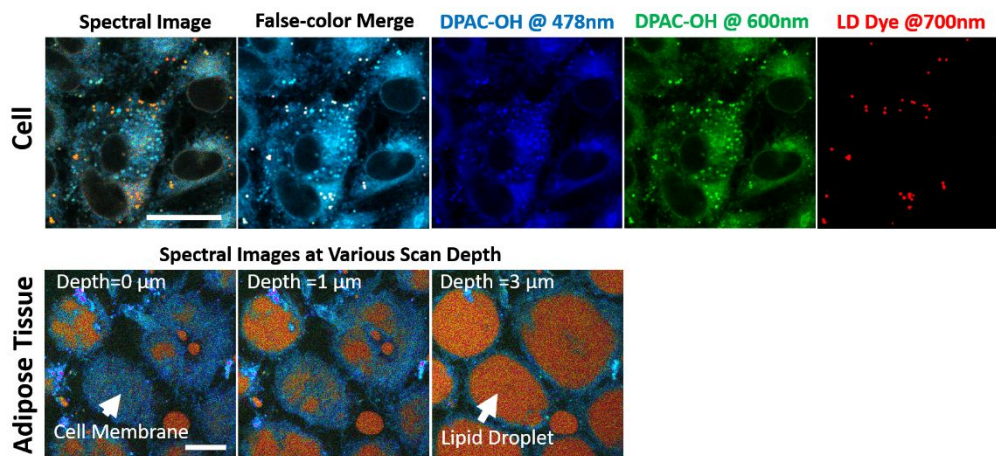


Figure S9. The co-localized results of DPAC-OH and lipid droplets (LDs) labeled HeLa cells and adipose tissue. The DPAC-OH labeled LDs exhibit orange color in the spectral images. Scale bar: 20 μm .